

Shanidar 10: A Middle Paleolithic immature distal lower limb from Shanidar Cave, Iraqi Kurdistan

Libby W. Cowgill^a, Erik Trinkaus^{a,*}, Melinda A. Zeder^b

^a Department of Anthropology, Campus Box 1114, Washington University, St. Louis, MO 63130, USA

^b Archaeobiology Program, National Museum of Natural History, Smithsonian Institution, Washington, DC 20560, USA

Received 1 June 2006; accepted 14 April 2007

Abstract

The analysis of the faunal remains from Shanidar Cave has identified an incomplete immature human distal leg and foot from the deepest levels of the Middle Paleolithic of Shanidar Cave, Iraq. The distal tibia, fibula, first metatarsal, and two tarsals, designated Shanidar 10, derive from a 1–2-year-old infant. The tibia exhibits a transverse line from a stress episode during the last quarter of its first year postnatal. The cross-sectional geometry of the tibial midshaft reveals modest cortical thickening and a level of diaphyseal robusticity similar to those of recent human infants of a similar developmental age.

© 2007 Elsevier Ltd. All rights reserved.

Keywords: Human paleontology; Late Pleistocene; Tibia; Metatarsal; Neandertal; Modern human

Introduction

Excavations at Shanidar Cave, in Iraqi Kurdistan (36° 50' N, 44° 13' E) by R.S. Solecki in 1953, 1957, and 1960 yielded a long Middle Paleolithic to modern archeological sequence, including the remains of nine Neandertal partial skeletons from the Middle Paleolithic Layer D (Solecki, 1963, 1971; Trinkaus, 1983). Excavation at Shanidar Cave has not continued since 1960, even though the archeological and human paleontological remains have become an important component of discussions of Middle Paleolithic human evolution in southwestern Asia.

In this context, there has been little attention paid to the Middle Paleolithic faunal remains from Shanidar Cave, all of which were transported to the USA. The faunal remains from Shanidar received only brief mention initially (Reed and Braidwood, 1960; Perkins, 1964) and a more detailed analysis of the Middle Paleolithic sample subsequently (Evins, 1981). However, with the transfer of the American Shanidar Cave collections to the

Smithsonian Institution in 2000, a more systematic sorting, identification, and taphonomic analysis of the Shanidar faunal remains has been undertaken, under the direction of MAZ (Zeder, 2005, 2006). In the course of this analysis, a sedimentologically conjoined set of distal leg and pedal bones (Excavation number II 920 D, SC 225) was identified in the Middle Paleolithic faunal remains as that of an immature human. Given its excavation in 1957 (field season II), and following on the previously numbered nine Shanidar Pleistocene humans, this specimen becomes Shanidar 10. This report is a description and paleobiological analysis of these immature appendicular Middle Paleolithic human remains. The goals of this paper are twofold: first, to describe the previously unknown Shanidar 10 material, including evidence for paleopathology, and second, to assess the one aspect of Shanidar 10 that might shed light on its paleobiology, its tibial diaphyseal robusticity in the context of Late Pleistocene and modern human subadult skeletal variation.

Context and geological age

The collection of faunal remains, with which Shanidar 10 was excavated, is from square D7 + E7 in Layer D in the

* Corresponding author. Tel./fax: +1 314 935 5207.

E-mail addresses: lwcowgil@artsci.wustl.edu (L.W. Cowgill), trinkaus@artsci.wustl.edu (E. Trinkaus), zederm@si.edu (M.A. Zeder).

main excavation trench of Shanidar Cave at a depth of 8.67–8.84 m below datum. This makes it, in stratigraphic terms, the oldest of the Shanidar human remains. The formerly known partial skeletons cluster into two stratigraphic horizons, one near the top of Layer D and one in the middle of Layer D. The former sample (Shanidar 1, 3, and 5) spans between 4.3 and 5.4 m below datum, whereas the latter sample (Shanidar 2, 4, 6, 7, 8, and 9) is between 7.2 and 7.9 m below datum [note that Shanidar 4, 6, 8, and 9 constituted a multiple (probably sequential) burial, in which Shanidar 4 was on top, at 7.5 m below datum].

Among these remains, the two highest specimens, Shanidar 1 and 5, exhibit craniofacial configurations close to those of Levantine and European “classic” oxygen isotope stage (OIS) 3 Neandertals. Two radiocarbon charcoal samples taken from 5.1 m below datum, between Shanidar 1 and 5 and the slightly deeper Shanidar 3, yielded conventional ^{14}C determinations of $46,900 \pm 1500$ (GrN-2527) and $50,600 \pm 3000$ (GrN-1495) (Vogel and Waterbolk, 1963). Preliminary results from ongoing efforts by MAZ to AMS radiocarbon date the Shanidar sequence support the conclusion that the upper portion of Layer D was $\geq 40\text{--}50$ ka ^{14}C BP. These dates and the cranial morphology of Shanidar 1 and 5 are probably sufficient to assign these remains to OIS 3, but more precise geological ages for the specimens will require additional radiometric dating of excavated remains.

The stratigraphically older human remains (especially Shanidar 2 and 4) have more “archaic” craniofacial configurations, similar to those of earlier OIS 5 or OIS 6 “early” Neandertals (Trinkaus, 1983, 1995). There are no radiometric dates for these deeper levels of Layer D, but new AMS dates confirm Solecki’s initial impression that all of the deposits below about 6 m in the cave are beyond the ca. 50,000 detection limit of radiocarbon. Based on the depth of deposits below this level, Solecki (1963) suggested an age of 60,000–70,000 BP for the middle of Layer D and an age of ca. 100,000 BP for its bottom. Given advances in Quaternary paleoclimatic sequences since the 1960s and the tenuous nature of any such inferences based on cave sediments, these ages for the deeper portions of Layer D should be considered only suggestive. However, it would be reasonable, using the morphological “dating” provided by the Shanidar 2 and 4 remains and Solecki’s inferences, to suggest that the lower part of Layer D dates to prior to OIS 3. All of the Layer D lithic assemblage is technotypologically Middle Paleolithic (Skinner, 1965; Akazawa, 1975), which constrains it to be no older than later Middle Pleistocene in age (Bar-Yosef, 1998; Barkal et al., 2003).

Given these considerations, Shanidar 10, at approximately a meter below the oldest of the formerly discovered remains (Shanidar 7 at 7.9 m), can be conservatively dated to OIS 6–4. In any case, it is likely to be older than the Levantine Neandertal remains from Amud, Dederiyeh, and Kebara (Valladas et al., 1987, 1999; Akazawa et al., 2002) but similar in age to or younger than those from Layers B and C at Tabun (Mercier and Valladas, 2003; Coppa et al., 2005).

The Shanidar 10 immature tibia, fibula, tarsals, and metatarsal

Shanidar 10 consists of a small (7.57 g) block of five bones (Fig. 1) held together by a hard, grayish carbonate matrix. Little would be gained by separating them (which would require both acidic and mechanical treatment), and one would risk shattering the smaller bones and damaging the surfaces. They are therefore left as a unit. The block contains the distal half of an immature tibia with most of the distal metaphysis, an associated fibular diaphysis without metaphyses, one side of a metatarsal retained on the matrix surface, a small and rounded immature bone that probably represents the early ossification stage of a distal tarsal, and part of the surface of another probable distal tarsal.

Distal left tibia

The tibia (maximum preserved length: 59.5 mm) retains the complete diaphyseal circumference from near midshaft to the distal metaphysis. There is no trace of a nutrient foramen, subperiosteally or within the cortical bone, as would be expected given the location of this feature proximal of midshaft in more complete specimens. The proximal fracture is transverse across the posterior half, and then it dips slightly distally anteriorly to the anterior crest. There is a small chip of bone on the anteromedial fracture’s margin, 2.5 mm wide and 1.0 mm proximodistal, that has been pushed endosteally slightly from the surface. The fracture reveals a small lamina of trabecular bone along 4.7 mm of the endosteal surface of the anteromedial shaft extending from the fracture distally. The remainder of the diaphysis, proximal of the distal metaphyseal trabeculae, appears to have been free of trabecular bone except for a couple of very small spicules (Fig. 2).

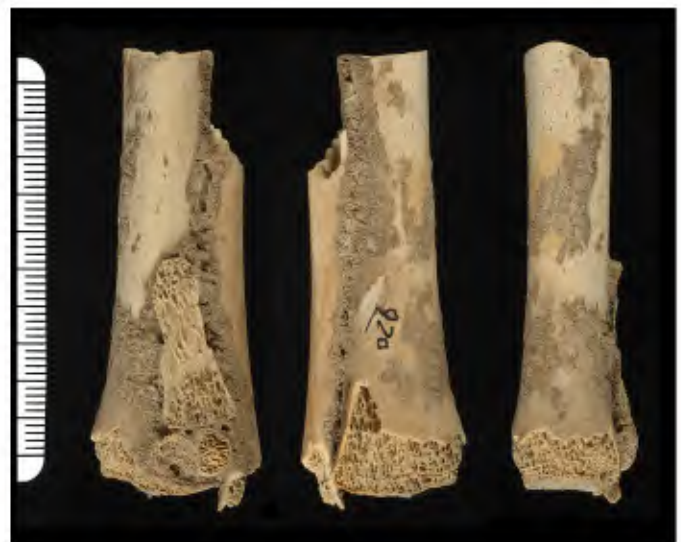


Fig. 1. Anterior, posterior, and medial views of the Shanidar 10 distal tibia, with the fibula, tarsals, and metatarsal evident in the anterior view and the fibula evident in the posterior view. Scale in millimeters.



Fig. 2. Anteroposterior and lateromedial radiographs of the Shanidar 10 distal tibia, with superimposition of the adherent left fibular diaphysis. The arrow points to the transverse line on the distal tibia.

The distal metaphysis has sustained abrasion around its entire circumference except on the extreme lateral portion. The degree of flare of the distal metaphysis is unknown, but it is most obvious posteromedially, where it is intact and protected by the matrix. The remaining metaphyseal surface is 10.3 mm anteroposterior by 17.8 mm mediolateral; visual continuation of the preserved distal subperiosteal contours suggests that the overall dimensions of the metaphysis probably approached 15–16 mm anteroposteriorly and 20–24 mm mediolaterally.

The midshaft cross section is subtriangular. The posterior diaphysis is transversely convex, and there is a clear but modest anterior crest (or border) forming a distinct angle between a flattened anteromedial surface and a rounded anterolateral surface. Anterodistally, the anterolateral surface is relatively broad and flat to slightly transversely concave, whereas the anteromedial surface is distinctly convex with a blunt ridge leading from the anterior diaphyseal crest onto the anteromedial metaphyseal border. What remains of the posterodistal diaphysis is evenly convex, with the margins becoming less distinct and more rounded distally.

The preserved portion of the distal metaphyseal surface is gently irregular and smooth, partly obscured in a thin layer of matrix, more proximal on the medial side, and angled in the coronal plane ca. 85° relative to the diaphyseal axis. There is no trace of the distal epiphysis, although it should probably have begun ossification by the inferred age (see below) of the individual (Scheuer and Black, 2000). However, it would have been small and indistinct and could have been easily destroyed, lost, or not recognized if not adherent to the metaphysis.

Distal left fibular diaphysis

Adherent to the tibia is a narrow, tubular bone lacking epiphyses/metaphyses (maximum preserved length: 51.7 mm); the

preserved ends sustained recent (excavation) damage as indicated by the fresh breaks of the bone. The bone is generally amorphous in its features, but given its preserved size, position, and morphology, it is identified as the diaphysis of the left fibula associated with the tibia. The orientation of the bone cannot be assessed from its external contours, and it has twisted axially relative to the tibia during decomposition and fossilization. However, the canal within the cortical bone for the nutrient artery is preserved on the surface that is posterior relative to the tibia; since the nutrient foramen is normally midmedial, the bone has rotated ca. 90° relative to the tibia, and its anatomical posterior margin is now facing largely lateral relative to the tibia. The planes of reference are therefore with respect to this approximate orientation using the nutrient canal.

The proximal end is fractured obliquely anteroproximal to posterodistal, and the distal end is fractured posteroproximal to anterodistal. The proximal fracture reveals only cortical bone and medullary cavity, but the distal fracture consists largely of trabecular bone with a ring of thinner cortical bone. Given the normal presence of the nutrient foramen near midshaft, and the trabecular-cortical configuration of the distal end indicating that it is close to the metaphyseal surface, the bone probably represents most of the distal half of the diaphysis, from near midshaft to above the distal metaphyseal surface.

The fibular diaphysis is ovoid in cross section towards midshaft, with a hint of an angulation posteromedially. However, that angle is an artifact of surface-bone loss on the posterior half of the medial side. Diameters, approximate given matrix and adherence to the tibia, are ca. 5.9 mm anteroposterior and ca. 5.5 mm mediolateral. As it continues distally, the shaft is straight along its anterior and posterior margins, but the lateral side is slightly concave, giving the impression of a minimal medial bowing of the bone. By the suprametaphyseal region distally, the cross section becomes largely round, with both anteroposterior and mediolateral diameters ca. 6.2 mm.

Left first metatarsal

Adherent to the matrix between the distal tibia and the fibular diaphysis is one side of an immature first metatarsal (maximum preserved length: 22.2 mm) (Fig. 3). The endosteal surface of the diaphysis is exposed, revealing the proximal metaphyseal trabeculae, the line of the proximal metaphysis, the distal epiphyseal trabeculae, and the contour of the distal subchondral bone. The subperiosteal surface is hidden within the matrix, and the hardness of the matrix and the fragility of the bone mean that it cannot be removed without risk of shattering the bone.

The bone is identified as a first metatarsal based on the contours of the proximal end and especially the distal contour of the preserved bone. The proximal contour is mildly convex. This fits the presence of a proximal epiphysis on the first metatarsal. Although it could also fit the immature contours of at least the middle three metatarsals, the parasagittal contour of the distal subchondral bone is strongly convex with dorsal and plantar notches; this is incompatible with the metaphyseal

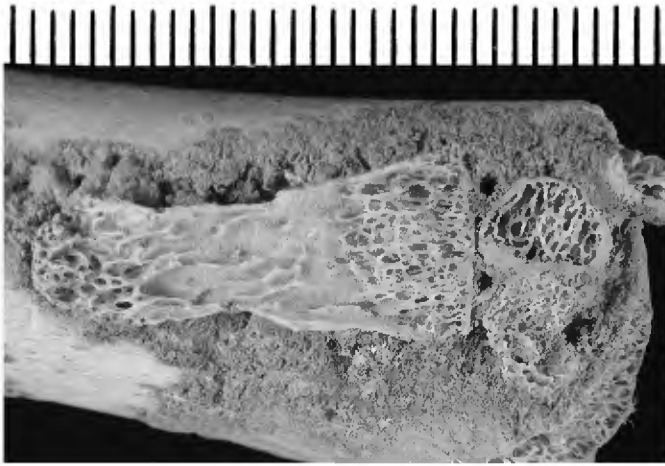


Fig. 3. Detail view of the Shanidar 10 first metatarsal and the two partial tarsal bones. The more complete but smaller tarsal (medial cuneiform?) is to the superior right of the metatarsal base, whereas the larger but less complete tarsal (lateral cuneiform?) is inferior of the first one. Scale in millimeters.

surfaces of the more lateral metatarsals. It is not possible to determine which of the preserved sides of the diaphysis is dorsal versus plantar, given damage to the edges. Therefore, whether it is the medial or lateral diaphysis is not assessable from the visible portions of the bone. While the height of the dorsoplantar base is 9.4 mm and the height of the dorsoplantar head is 7.1 mm, both of these measurements represent only the preserved portion of the specimen, and they should not be interpreted as articular (or metaphyseal) dimensions. The bone is identified as left on the basis of its association with the left tibia.

Left distal tarsal bone

Adjacent to the base of the first metatarsal is the abraded side of a subspherical bone, consisting of trabeculae with a thin cortical subchondral surface (maximum diameter: ca. 6.5 mm; maximum observable breadth: ca. 6.0 mm) (Fig. 3). This bone, based on position and size, represents one of the distal tarsals, of which the medial cuneiform seems most likely given its proximity to the base of the first metatarsal. The sequence of ossification of the cuneiform bones is lateral, then medial, then intermediate, with the first appearing by ca. 6 months postnatal, the second present by one year postnatal, and the third by the second year postnatal (Scheuer and Black, 2000). The bone is at an early, amorphous stage of ossification, which makes it likely (see age estimate below) that it represents the medial cuneiform if the individual was closer to one year of age and the intermediate cuneiform if the individual was in advance of two years of age.

Left distal tarsal bone or epiphysis

On the anterior surface of the specimen, between the probable medial cuneiform and the distal tibia, are the internal surface of the outer cortical shell and the exposed trabeculae of

another distal tarsal bone or an epiphysis (Fig. 3). Relative to the planes of the tibia, it is 6.5 mm wide and 5.5 mm high. It is probably part of another distal tarsal bone, since both the distal tibial epiphysis and the first metatarsal proximal epiphysis would be relatively flat and this was part of a subspherical bone. It could be part of the intermediate cuneiform, but given its degree of ossification and original dimensions that would have made it larger than the more complete tarsal identified as the medial cuneiform, it is more likely to be part of the lateral cuneiform.

Separateness from Shanidar 7

It is necessary to address whether the bones here attributed to Shanidar 10 could derive from Shanidar 7, the Neandertal infant recovered from deposits about 1 m above and 3 to 4 m to the northeast of Shanidar 10. While the only tibial piece from Shanidar 7 is a diaphyseal section of indeterminate side, Shanidar 7 preserves both first metatarsals, including a complete left one, an element also found in Shanidar 10. Moreover, intermetaphyseal length of the Shanidar 10 first metatarsal (ca. 22.5 mm, based on its maximum preserved length of 22.2 mm) is 23.6% longer than the Shanidar 7 value (18.2 mm); this length difference would produce a level of length asymmetry exceptional within normal limb bones (Trinkaus et al., 1994; Čuk et al., 2001). These considerations therefore confirm that the Shanidar 10 bones cannot derive from the Shanidar 7 skeleton.

Age-at-death estimation

The Shanidar 10 lower-limb bones represent those of an infant during the first couple of years postnatal, based on morphology and general bone maturity. There are no accurate age indicators preserved on the specimen, and the absence of epiphyses is merely the absence of evidence. The best age indicator, despite associated difficulties, is the estimated length of the tibia.

The intermetaphyseal tibial length can be estimated by doubling the distance from the proximal fracture to the distal metaphysis. The proximal fracture is close to midshaft, as indicated by the clear anterior crest present at the fracture, which occurs primarily in the middle of the diaphysis. The resultant intermetaphyseal length is therefore ca. 120 mm.

Several different methods of estimating age based on tibial intermetaphyseal length are available, but each one is associated with difficulties. Gindhart (1973) developed age standards based on tibial length using radiographs of subjects from the Fels Research Institute longitudinal study. Following Gindhart (1973), a tibial intermetaphyseal length of ca. 120 mm provides an age estimate of 0.75–1.50 years postnatal (the same for males and females). This estimate, however, is based on a reference sample comprised of individuals of northwestern European descent, who likely possessed temperate-climate body proportions. If Shanidar 10 had relatively short tibiae, as did many Neandertals, including the slightly stratigraphically younger Shanidar 2 and 6 adults (Trinkaus, 1981; Trinkaus

and Ruff, 1999b), then the individual's age would be underestimated. The same would apply if the population had relatively short stature compared to the Euro-American reference sample, a likely pattern given Neandertal adult stature estimations (Trinkaus, 2006).

Thus, it is more appropriate to estimate age based on a smaller-bodied, cold-adapted sample. Accordingly, the age of Shanidar 10 was also estimated using a regression formula developed from a sample of Inuit infants and juveniles from the site of Point Hope, Alaska (ages 0–4 years, $n = 14$). Using a tibial intermetaphyseal length of 120 mm as the independent variable, a slightly older age estimate of 1.71 ± 0.27 years is produced [$\text{age} = (\text{TIB} - \text{IML} \times 0.042) - 3.34$, where TIB = tibial length and IML = intermetaphyseal length; $p < 0.001$, $r^2 = 0.949$]. While this regression formula is based on a limited number of individuals, it may provide a more accurate age estimate for Shanidar 10 given the likelihood that this individual was from a population characterized by both shorter stature and lower crural indices than the Euro-American sample of Gindhart (1973).

In addition, the tibial and first metatarsal intermetaphyseal lengths of Shanidar 10 are compared in Table 1 to the available data for western Asian and European Middle Paleolithic immature individuals in order to provide an additional comparative framework for age estimation. The Shanidar 10 tibial and first metatarsal lengths fall above those for Kiik-Koba 2 and Shanidar 7 (ages <1.0 years), and they are similar to or slightly below those for Dederiyeh 1 and 2, La Ferrassie 6, and Roc de Marsal 1 (ages >1.5 years). They are also below those for Qafzeh 21 and Skhul 1, but Skhul 1 is likely to have had a relatively long tibia given the neotropical body proportions of the Qafzeh-Skhul sample (Trinkaus and Ruff, 1999a,b; Holliday, 2000). These comparisons to two modern reference samples and Middle Paleolithic subadults from southwestern Asia and Europe put the best estimate of age at death for Shanidar 10 at between approximately one and two years postnatal. Given the uncertainty of estimating subadult age based on intermetaphyseal length, however, it

remains possible that the Shanidar 10 individual's actual age was moderately outside of this range.

Paleopathology

The Shanidar 10 remains do not exhibit any external pathological lesions, but radiographically, there is a distinct transverse (“Harris”) line present in the distal metaphysis of the tibia, located 8.5 mm from the metaphyseal surface (Fig. 2). Although thin, it is continuous anteroposteriorly and mediolaterally through the trabeculae and therefore represents a growth-arrest line.

In order to infer the age at which this stress episode likely occurred, it is first necessary to calculate the metaphyseal length at the time of insult. Differential growth occurs at the proximal and distal tibial metaphyses, resulting in approximately 57% of tibial growth occurring at the proximal end (Anderson et al., 1963). Following this, the total intermetaphyseal length at the time of insult was ca. 100 mm. Using a modern Euro-American standard (Gindhart, 1973), this length indicates an age of insult between about 4 and 9 months postnatal, but probably a little older given the generally shorter tibiae of the Late Pleistocene infant and juvenile remains (Table 1). The regression formula of age on intermetaphyseal tibia length derived from the Inuit sample (see above) yields an age of ca. 10 months postnatal. Alternatively, an estimated 20 mm of growth between the time of insult and death implies (following Gindhart, 1973) over seven months of growth, suggesting that the growth-arrest line occurred between seven and eight months prior to the death of Shanidar 10.

It is difficult to compare such lines across samples due to several well-documented complications in the interpretation of Harris lines. These complications include high levels of line resorption, large intra- and interobserver line-counting errors, a lack of a 1:1 correspondence between lines and stress episodes, and the general mortality bias in archeological samples towards individuals who did not survive until adulthood (Gindhart, 1964; Macchiarelli et al., 1994; Lewis and Roberts,

Table 1

Tibial and first metatarsal intermetaphyseal lengths (IML) compared to those of infant and juvenile Middle Paleolithic humans (with estimated values indicated in parentheses)

Specimen	Developmental age	Tibia IML	MT1 IML	Reference
Shanidar 10	—	ca. 120	22.2	
<i>Neandertals</i>				
Kiik-Koba 2	0.4–0.5	(78)	—	Vlček, 1973
Shanidar 7	0.75	—	18.2	Trinkaus, 1983
Dederiyeh 1	1.6–2.5	128.6	(26.4)	Dodo et al., 2002; Kondo and Dodo, 2002
Dederiyeh 2	1.8–2.5	(109)	—	Ishida and Kondo, 2002; Kondo and Ishida, 2002
Roc de Marsal 1	2.5–4.0	(130)	(24.7)	Madre-Dupouy, 1992
La Ferrassie 6	3.0–5.0	129	—	Heim, 1982
<i>Early modern humans</i>				
Qafzeh 21	ca. 3.0	—	25.6	Tillier, 1999
Skhul 1	ca. 4.5	156	26.5	McCown and Keith, 1939; Trinkaus, personal measurement

1997). However, for comparative purposes, it is useful to examine the frequency of transverse-line formation in other Late Pleistocene immature remains and in more recent samples. Among the Late Pleistocene immature tibiae, the Dederiyeh 1 and 2 and Roc de Marsal 1 tibiae are too damaged (Madre-Dupouy, 1992; Kondo and Dodo, 2002; Kondo and Ishida, 2002), and the two Skhul 1 tibiae and the La Ferrassie 6 tibia lack transverse lines (Trinkaus, personal observation). However, the Lagar Velho 1 distal right tibia has two lines, at approximately 1% and 10% of its intermetaphyseal length (Trinkaus et al., 2002b).

The distal tibiae of individuals between 0.5 and 3.0 years in the pooled recent human comparative sample with sufficiently clear radiographs ($n = 54$) were inspected for Harris lines, defined for this analysis as any line crossing at least half of the diaphysis (Gindhart, 1964; Hummert and Van Gerven, 1985; Mays, 1985). The sample was scored twice by LWC and then checked for consistency to reduce intraobserver error, and limited to individuals aged three years and under to mitigate the effects of remodeling. Within this age group, 52% of individuals showed some type of transverse line, although only 45% of the lines counted crossed the entire distal tibial metaphysis. Of the individuals that did display lines prior to the age of three, the majority of them were similar to the Shanidar 10 tibia in having a single line (58%). When the age of insult is estimated, 55% of all lines were produced between birth and one year. While it is difficult to draw conclusions regarding the health status of an individual based on a single element, the Shanidar 10 tibia is not unusual in possessing a single transverse line for its general time period and developmental stage.

Human group attribution

Since southwestern Asia was occupied during the Middle Paleolithic by both late archaic (Neandertal) and early modern humans, it is of interest to know whether Shanidar 10 can be assigned to one of these groups. Aside from general taxonomic attribution, the contrasts in body proportions between these two groups, mature and immature (Trinkaus and Ruff, 1999a,b; Tillier, 1999; Holliday, 2000), means that the assignment of Shanidar 10 to a group has implications for any appropriate scaling of its tibial diaphyseal robusticity (Ruff et al., 1993).

The late archaic/Neandertal lineage is well documented through Layer D of Shanidar Cave (Trinkaus, 1983) and in Layers C and B of Tabun Cave, and chronologically more recent Neandertal remains have been recovered from the Amud, Dederiyeh, and Kebara caves of the eastern Mediterranean littoral (McCown and Keith, 1939; Suzuki and Takai, 1970; Bar Yosef and Vandermeersch, 1991; Hovers et al., 1995; Akazawa and Muhesen, 2002; see Trinkaus, 1984; Stefan and Trinkaus, 1998). This association would argue for late archaic/Neandertal lineage affinities for Shanidar 10.

However, there were also early modern humans at Qafzeh and Skhul near and on the southern portion of the eastern Mediterranean littoral during the middle of OIS 5 (McCown and Keith, 1939; Vandermeersch, 1981; Tillier, 1999; Grün et al., 2005). It is unclear whether these early modern humans,

probably recently derived from OIS 6–5 east African populations (Trinkaus and Ruff, 1999a,b; Holliday, 2000), penetrated into southwestern Asia beyond the region of Qafzeh and Skhul, and therefore whether they reached the Zagros Mountains. Yet, at least at Qafzeh, the early modern humans are associated with Afro-Arabian faunal elements (Rabinovich and Tchernov, 1995; Tchernov, 1998), and the Middle Paleolithic fauna from Shanidar Cave is strictly Palearctic, including *Capra*, *Ovis*, *Cervus*, *Sus*, *Vulpes*, *Ursus*, and *Testudo* (Evins, 1981; Zeder, personal observation). This faunal contrast and the geographical context reinforce the view that Shanidar 10 should be included with Shanidar 1–9 in a southwest Asian Neandertal lineage. Shanidar 10 will therefore be considered here as an “early” Neandertal, closely aligned with Shanidar 4 and 6–9 and the Tabun Layer B remains.

Diaphyseal cross-sectional geometry

Materials and methods

The one aspect of the Shanidar 10 tibia that can be meaningfully, quantitatively compared across samples is the cross-sectional geometry of its exposed midshaft. The postmortem fracture of the tibia is sufficiently close to midshaft, perpendicular to the diaphyseal axis, and well-preserved to permit use of the fracture to quantify its diaphyseal properties. To this purpose, the fracture was photographed, projected enlarged onto a Summagraphics 1812 tablet, and digitized. From these data, cross-sectional parameters were computed using a PC version (Eschman, 1992) of SLICE (Nagurka and Hayes, 1980). The resultant values plus external diameters and cortical thicknesses are provided in Tables 2 and 3.

Combinations of these measurements were compared to data available for immature Late Pleistocene tibial midshafts, all ≤ 6 years of age (Table 3). These data were generated by one of us (ET) for La Ferrassie 6, Skhul 1, and Yamashita-cho 1, and published data were used for Dederiyeh 1 and 2 and Lagar Velho 1 (Trinkaus and Ruff, 1996; Kondo and Dodo, 2002; Kondo and Ishida, 2002; Trinkaus et al., 2002a). La Ferrassie 6 and Dederiyeh 1 and 2 are OIS 3 Neandertals, Skhul 1 is an OIS 5 modern human, and Lagar Velho 1 and Yamashita-cho 1 are OIS 3 modern humans.

To provide a broader context for these paleontological data, cross-sectional data for four recent human samples were employed (Table 4). An age range of 0.5 to 6.0 years

Table 2
Midshaft linear dimensions for the Shanidar 10 immature tibia (in millimeters)

Dimension	Value
Anteroposterior diameter	11.6
Mediolateral diameter	10.7
Anterior cortical thickness	2.9
Posterior cortical thickness	2.8
Anteromedial cortical thickness	1.7
Anterolateral cortical thickness	1.9
Posteromedial cortical thickness	2.5
Posterolateral cortical thickness	2.4

Table 3
Tibial midshaft cross-sectional parameters for Shanidar 10 and other Late Pleistocene immature humans (see text for abbreviations)

Specimen	TA ¹	CA ¹	I_x^2	I_y^2	I_{max}^2	I_{min}^2	J^2	θ
Shanidar 10 ³	86.0	59.3	(563.4)	(516.0)	615.3	464.1	1079.4	(126°)
La Ferrassie 6 ³	116.4	78.4	(1110.9)	(860.0)	1108.6	829.0	1970.9	(108°)
Dederiyeh 1 ⁴	133.1	96.0	1604.1	1056.0	—	—	2660.1	—
Dederiyeh 2 ⁵	80.7	36.3	396.0	232.0	—	—	628.0	—
Skhul 1	106.5	80.9	1006.2	735.4	1012.5	729.1	1741.6	81.5°
Lagar Velho 1 ⁶	158.6	88.8	1792.9	1495.2	1914.6	1373.5	3288.1	61.5°
Yamashita-cho 1	155.3	99.9	1958.0	1468.0	2037.0	1390.0	3426	69.6°

¹ Cross-sectional areas in mm².

² Second moments of area in mm⁴.

³ Given the absence of the proximal metaphyses of the Shanidar 10 and La Ferrassie 6 tibiae and their orientations based on diaphyseal morphology, the orientations of the bones relative to their anteroposterior and mediolateral axes may be slightly in error. For this reason, I_x , I_y , and θ are placed in parentheses, indicating their estimated natures.

⁴ Data from Kondo and Dodo (2002).

⁵ Data from Kondo and Ishida (2002).

⁶ Right and left values averaged; data from Trinkaus et al. (2002a).

of age was selected for the comparative material in order to provide a sufficiently narrow developmental window to be biologically relevant to the developmental stage of the Shanidar 10 specimen, but a broad enough range to both accommodate any potential error in the aging of the Late Pleistocene fossil remains and reveal any developmental trends. Three of the samples (Mistihalj, Indian Knoll, and Point Hope) are from nonurban, nonmechanized societies, with Indian Knoll and Point Hope being semisedentary foraging populations. The Dart Collection is an ethnically mixed, both urban and nonurban sample of native southern Africans. The developmental ages were assessed using crown and root formation following Smith (1991) and Liversidge and Molleson (2004) when mandibles were available (see Table 4 for percentages of samples dentally aged). Otherwise, age was assessed using a population-specific regression of age against femur length (Table 4).

The midshaft cross sections of the recent humans, plus those of La Ferrassie 6, Skhul 1, and Yamashita-cho 1, were reconstructed using polysiloxane molding putty (Cuttersil Putty Plus) to transcribe the subperiosteal contours and biplanar radiography to generate parallax-corrected cortical thicknesses, from which the endosteal contours were interpolated (O'Neill and Ruff, 2004). All were projected enlarged and digitized as was the Shanidar 10 cross section.

Comparisons involve cortical (CA) to total subperiosteal (TA) thickness (CA/TA) (Fig. 4), anteroposterior (I_x) versus mediolateral (I_y) second moments of area (I_x/I_y) (Fig. 5), maximum (I_{max}) versus minimum (I_{min}) second moments of area (I_{max}/I_{min}) (Fig. 6), and the polar moment of area (J) scaled to bone length adjusted for body shape (Fig. 7). The ratios of both sets of perpendicular second moments of area (I_x/I_y and I_{max}/I_{min}) are provided, since it is unclear which ratio more accurately reflects diaphyseal response to habitual loading during weight-bearing and locomotion in young individuals. Given that infant and juvenile tibial midshaft cross sections (including the Late Pleistocene specimens) approximate an equilateral triangle, the orientation of I_{max} (θ) varies largely in response to minor variations in cross-sectional shape; given that $\theta = 0^\circ$ for a mediolateral orientation of I_{max} and 90° for an anteroposterior orientation, the mean and standard deviation of θ are 90.5° and 31.4° , respectively, with a range of 19° to 143° across the pooled recent human samples, and the slope of θ is not significantly correlated with age (in years) ($r^2 = 0.019$, $p = 0.196$). The values of θ are moderately high for Shanidar 10 and La Ferrassie 6 but below recent human mean for the three early modern human immature tibiae (Table 3).

Polar moments of area in weight-bearing diaphyses should be scaled to beam length (or bone length) times body mass

Table 4
Descriptions and sample sizes of the modern comparative samples

Sample	Sample description	Location	<i>n</i>	Percentage dentally aged	Age vs. femur length r^2
Dart Collection	Twentieth-century ethnically mixed southern Africans	University of Witwatersrand, Johannesburg, South Africa	25	92.0%	0.890
Mistihalj	Medieval eastern Europeans from Serbia	Harvard Peabody Museum	15	100.0%	0.871
Indian Knoll	North American Archaic period Native Americans from Kentucky	University of Kentucky at Lexington	34	82.4%	0.901
Point Hope	Pre- and protohistoric Alaskan Inuits	American Museum of Natural History	14	92.9%	0.849
Total			88	88.6%	

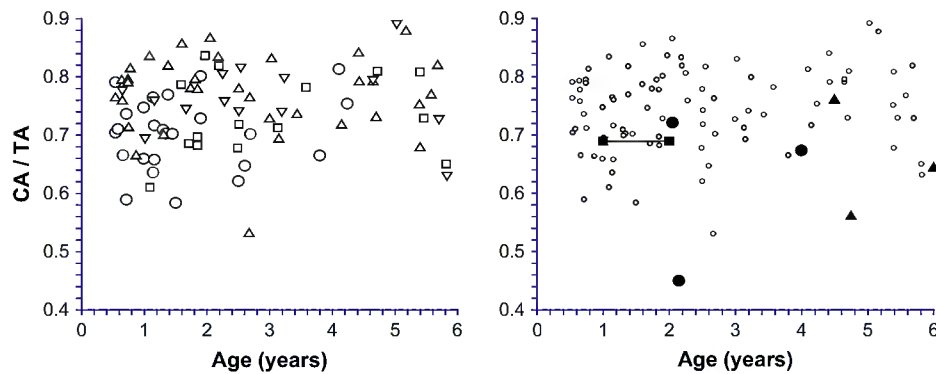


Fig. 4. Bivariate plots of tibial midshaft cortical area/total area (CA/TA) versus age for the recent human comparative samples (left) and the immature Late Pleistocene fossil human specimens together with the pooled recent human samples (right). In the recent human plot: circles = recent southern Africans; up triangles = prehistoric Native Americans; squares = medieval Europeans; down triangles = pre- and protohistoric Inuits. In the fossil human plot: connected black squares = Shanidar 10 values for 1- and 2-year age estimates; black circles = Neandertals; black triangles = early modern humans; small open circles = recent humans.

(Trinkaus and Ruff, 2000). However, body mass is difficult to estimate for immature skeletal remains and nearly impossible in a specimen as incomplete as Shanidar 10. Therefore, following Ruff et al. (1993), polar moments are divided by tibia length^{16/3} ($\times 10^8$) because they scale to that power in mature skeletal samples. However, as with adult Late Pleistocene humans (Trinkaus, 1981; Holliday, 1997a,b, 2000; Trinkaus and Ruff, 1999b), there is variation in immature tibiofemoral (or crural index) proportions and possibly in relative body breadths (Tompkins and Trinkaus, 1987; Ruff et al., 2002; Kondo and Ishida, 2002). Among the recent human samples, both the adult and immature Inuit remains from Point Hope exhibit relatively short tibiae in contrast to the other recent human samples (Cowgill, 2006; Holliday and Hilton, 2006), as with other Inuit samples (Trinkaus, 1981). It is not possible to directly assess body breadths for these immature individuals, but one can partially correct for the low crural indices in the Inuits and relevant fossil specimens (Dederiyeh 1 and 2, La Ferrassie 6, and Lagar Velho 1).

A correction is therefore not employed for variation in body breadth, since it is unknown, but a correction for the low crural indices of the Inuits, Neandertals, and Lagar Velho 1 is employed by multiplying tibial intermetaphyseal length by 1.05

(a 5% adjustment) (see Ruff et al., 1993). Therefore, following Ruff et al. (1993), the standardized polar moment of area (J-STD) becomes: $[J/(1.05 \times \text{TIB} - \text{IML}^4)^{4/3}] \times 10^8$, or $[J/(1.067 \times \text{TIB} - \text{IML}^{16/3})] \times 10^8$. The same correction is applied to Shanidar 10; the crural index of Shanidar 6 is relatively low (Trinkaus, 1983), and the Shanidar 2 tibial diaphysis can only have a reasonable level of robusticity if it possessed the abbreviated distal limb segments of other Neandertals (Trinkaus and Ruff, 1999b).

Cross-sectional bone distribution

The distributions of pooled recent human CA/TA and I_x/I_y (Figs. 4–6) show no significant change with age through the age span analyzed here (0.5–6.0 years), with r^2 values of 0.022 and 0.010, respectively ($p = 0.167$ and 0.552). The distribution of I_{\max}/I_{\min} suggests a slight increase with age ($r^2 = 0.050$, $p = 0.035$), but the p -value remains nonsignificant after a multiple-comparison correction. Moreover, the large variation in the orientation of $I_{\max}(\theta)$ (see above) makes the biomechanical significance of I_{\max}/I_{\min} values ambiguous. Dederiyeh 2 and Lagar Velho 1 have low relative cortical areas, as noted previously (Kondo and Ishida, 2002; Trinkaus

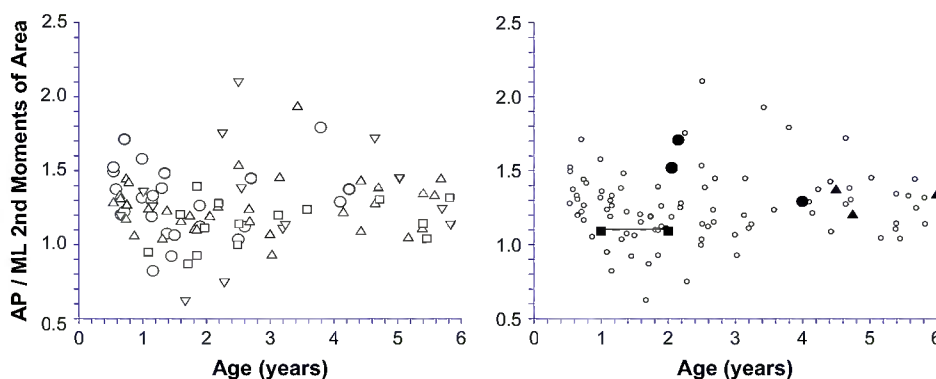


Fig. 5. Bivariate plots of tibial midshaft anteroposterior/mediolateral second moments of area (I_x/I_y) versus age for the recent human comparative samples (left) and the immature Late Pleistocene fossil human specimens together with the pooled recent human samples (right). Symbols as in Fig. 4.

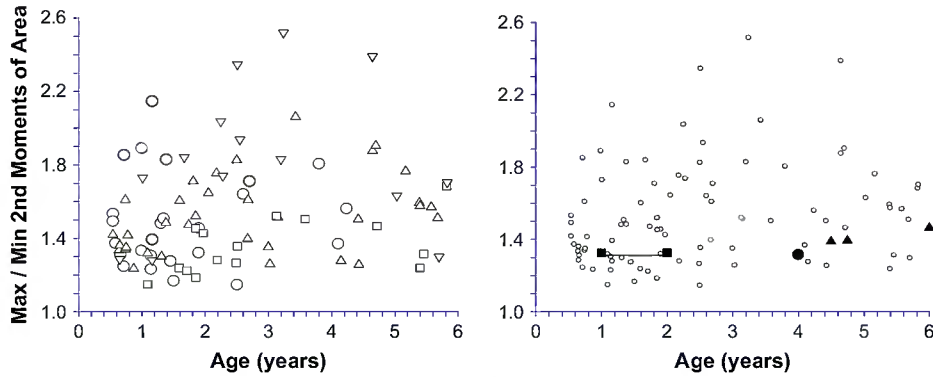


Fig. 6. Bivariate plots of tibial midshaft maximum/minimum second moments of area (I_{max}/I_{min}) versus age for the recent human comparative samples (left) and the immature Late Pleistocene fossil human specimens together with the pooled recent human samples (right). Symbols as in Fig. 4.

et al., 2002a). The remaining Late Pleistocene immature tibiae, including Shanidar 10, are unexceptional in their tibial midshaft percent cortical areas. Similarly, there is little difference in the I_x/I_y or I_{max}/I_{min} values across the recent human and fossil tibiae, although the two Dederiyeh specimens are moderately high in the I_x/I_y distribution (I_{max} and I_{min} are unavailable for Dederiyeh 1 and 2).

Diaphyseal robusticity

The standardized polar moments of area (J-STD) follow the pattern previously documented for immature femora (Ruff et al., 1994; Trinkaus and Ruff, 1996), in which there is a steady decrease in apparent robusticity through development related to the differential growth of body length and breadth (Fig. 7). There is little difference across the recent human samples. Four of the Late Pleistocene immature tibiae, Dederiyeh 1, La Ferrassie 6, Skhul 1, and Lagar Velho 1 (despite cranial-index corrections on all except Skhul 1, which reduce the apparent robusticity of the tibiae), cluster along the more robust margins of the recent human pooled distribution. Dederiyeh 2 and Shanidar 10, however, fall in the middle of the recent human distribution. In order for Shanidar 10 to fall with the other, more robust, immature fossil tibiae, it would have to be assigned an age of 3 to 4 years, which is unlikely given its tibial and metatarsal lengths. If Shanidar 10 were given

a higher cranial index, similar to the recent human samples, its J-STD value would become 0.894, as opposed to the low cranial-index value of 0.824 employed in Fig. 7; both values are well within the recent human distribution for its probable age range.

Due to the fact that the tibial intermetaphyseal length for Shanidar 10 was estimated, it is possible that standardizing the polar moment of area by length^{16/3} could result in compounding the estimation error and therefore bias the results of this analysis. In order to evaluate the impact that an error in the estimation of tibial length would have on the analysis of J-STD, the polar moment of area for Shanidar 10 was recalculated using lower (110 mm) and higher (130 mm) estimated values of tibial intermetaphyseal length instead of 120 mm. If a length estimate of 130 mm is used to standardize the polar moment of area, the resultant values for the higher and lower cranial-index scaling are 0.583 and 0.538, respectively. Both values fall towards the lower limits of the recent human range of variation. Given that the other Late Pleistocene values for J-STD are well within or are at the upper margin of the Holocene human distribution, a length estimate of 130 mm for the Shanidar 10 tibia is probably too high. If an estimate of 110 mm is used, however, the J-STD values for Shanidar 10 become 1.523 and 1.404 for the higher and lower cranial-index adjustments, respectively. These points are higher within the distribution of modern human values and close to the value

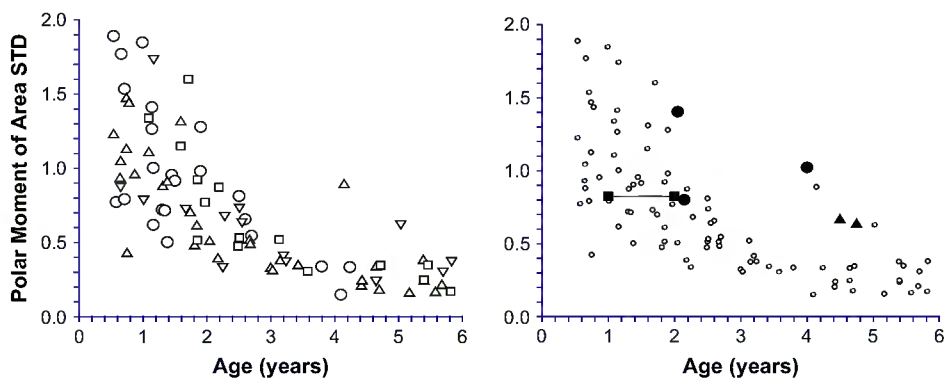


Fig. 7. Bivariate plots of tibial midshaft standardized polar moment of area (see text for calculation) versus age for the recent human comparative samples (left) and the immature Late Pleistocene fossil human specimens together with the pooled recent human samples (right). Symbols as in Fig. 4.

for Dederiyeh 1. However, only the attribution of a relatively high crural index and especially an age at death close to two years postnatal would place Shanidar 10 along the more robust limits of the recent human samples, close to the values for Dederiyeh 1, La Ferrassie 6, Skhul 1, and Lagar Velho 1.

As with Dederiyeh 1 and 2, the reasonable range of robusticity values for Shanidar 10 documents the developmental variability of these Late Pleistocene human remains. Yet, at an estimated age between 1 and 2 years postnatal, it is unclear whether Shanidar 10 (or Dederiyeh 2) had made the developmental transition to full bipedal walking and hence to full loading of the tibia in posture and locomotion, which generally occurs in recent human children between twelve and fifteen months postnatal (Gesell and Thompson, 1934; Shirley, 1963; Bly, 1994). Ruff (2003), using subadult cross-sectional properties derived from a recent Euro-American longitudinal growth study, detected a rapid increase in femoral strength between the ages of one and two years postnatal, which was associated with a sudden decrease in humeral strength. This pattern was interpreted as a response to the change in locomotor patterns as the infants transitioned between crawling and walking, no longer using the humerus as a primary weight-bearing element and shifting the entirety of their body mass to the lower limb (Ruff, 2003). Given its limited weight-bearing function in crawling, the tibia would be expected to show a similar strength increase following the onset of bipedal walking. It may well be that the locomotor transition was largely complete in Dederiyeh 1 (and the older individuals), but that it was less advanced in the potentially younger Dederiyeh 2 and Shanidar 10 individuals, resulting in their relatively lower J-STD values when compared to older Late Pleistocene specimens in the context of modern human variation. This would argue for similarity in the developmental baseline levels of lower-limb strength across Late Pleistocene and recent humans, with a shift towards more robust femora and tibiae in the earlier samples only after walking was fully established.

Conclusion

The Shanidar 10 distal lower limb adds to our sample of immature Neandertal remains from southwestern Asia. In conjunction with that of a small number of other Late Pleistocene infant and early juvenile remains, the diaphyseal cross-sectional geometry of Shanidar 10 suggests that Late Pleistocene humans may have had levels of lower-limb hypertrophy similar to those of most recent humans prior to the age of full developmental bipedality, and that the robusticity evident among the adults only emerged subsequently.

Acknowledgments

The collection of comparative recent and Late Pleistocene human data was funded by NSF SBR-9318702, the Leakey Foundation, the Wenner-Gren Foundation, the Japan Society for the Promotion of Science, and Washington University (to ET) and the Leakey Foundation, NSF BCS-0549925, and

Washington University (to LWC). To them and the curators who made specimens available, we are grateful.

References

- Akazawa, T., 1975. Preliminary notes on the Middle Palaeolithic assemblage from the Shanidar Cave. *Sumer* 31, 3–10.
- Akazawa, T., Muhesen, S. (Eds.), 2002. Neandertal Burials. Excavations of the Dederiyeh Cave, Afrin, Syria. Neanderthal Research Center for Japanese Studies, Kyoto.
- Akazawa, T., Muhesen, S., Dodo, Y., Ishida, H., Konda, O., Yoneda, M., Griggo, C., 2002. A summary of the stratigraphic sequence. In: Akazawa, T., Muhesen, S. (Eds.), Neandertal Burials. Excavations of the Dederiyeh Cave, Afrin, Syria. International Research Center for Japanese Studies, Kyoto, pp. 15–32.
- Anderson, M., Green, W.T., Messner, A.M.B., 1963. Growth and predictions of growth in the lower extremities. *J. Bone Joint Surg.* 45, 1–14.
- Barkal, R., Gopher, A., Lauritzen, S.E., Frumkin, A., 2003. Uranium series dates from Qesem Cave, Israel, and the end of the Lower Palaeolithic. *Nature* 423, 977–979.
- Bar-Yosef, O., 1998. The chronology of the Middle Paleolithic of the Levant. In: Akazawa, T., Aoki, K., Bar-Yosef, O. (Eds.), Neandertals and Modern Humans in Western Asia. Plenum, New York, pp. 39–56.
- Bar Yosef, O., Vandermeersch, B. (Eds.), 1991. *Le Squelette Moustérien de Kébara 2*. Éditions du C.N.R.S., Paris.
- Bly, L., 1994. Motor Skills Acquisition in the First Year. *Therapy Skill Builders*, Tucson.
- Coppa, A., Grün, R., Stringer, C., Eggins, S., Vargiu, R., 2005. Newly recognized Pleistocene human teeth from Tabun Cave, Israel. *J. Hum. Evol.* 49, 301–315.
- Cowgill, L.W., 2006. Postcranial growth and development of immature skeletons from Point Hope, Alaska. *Am. J. Phys. Anthropol.* 42 (Suppl.), 78.
- Čuk, T., Leben-Seljak, P., Štefančič, M., 2001. Lateral asymmetry of human long bones. *Var. Evol.* 9, 19–32.
- Dodo, Y., Kondo, O., Nara, T., 2002. The skull of the Neandertal child of burial No. 1. In: Akazawa, T., Muhesen, S. (Eds.), Neandertal Burials. Excavations of the Dederiyeh Cave, Afrin, Syria. International Research Center for Japanese Studies, Kyoto, pp. 93–138.
- Eschman, P.N., 1992. SLOMM Version 1.6. Eschman Archaeological Services, Albuquerque.
- Evins, M.A., 1981. A study of the fauna from the Mousterian deposits at Shanidar Cave, northeastern Iraq. M.A. Thesis, University of Chicago.
- Gesell, A., Thompson, H., 1934. *Infant Behavior: Its Genesis and Growth*. McGraw-Hill, New York.
- Gindhart, P.S., 1964. The frequency of appearance of transverse lines in the tibia in relation to childhood illnesses. *Am. J. Phys. Anthropol.* 31, 17–22.
- Gindhart, P.S., 1973. Growth standards for the tibia and radius in children aged one month through eighteen years. *Am. J. Phys. Anthropol.* 39, 41–48.
- Grün, R., Stringer, C., McDermott, F., Nathan, R., Porat, N., Robertson, S., Taylor, L., Mortimer, G., Eggins, S., McCulloch, M., 2005. U-series and ESR analyses of bones and teeth relating to the human burials from Skhul. *J. Hum. Evol.* 49, 316–334.
- Heim, J.L., 1982. *Les Enfants Néandertaliens de La Ferrassie*. Masson et Cie, Paris.
- Holliday, T.W., 1997a. Body proportions in Late Pleistocene Europe and modern human origins. *J. Hum. Evol.* 32, 423–447.
- Holliday, T.W., 1997b. Postcranial evidence of cold adaptation in European Neandertals. *Am. J. Phys. Anthropol.* 104, 245–258.
- Holliday, T.W., 2000. Evolution at the crossroads: modern human emergence in western Asia. *Am. Anthropol.* 102, 54–68.
- Holliday, T.W., Hilton, C.E., 2006. Body proportions of the Point Hope sample. *Am. J. Phys. Anthropol.* 42 (Suppl.), 105.
- Hovers, W., Rak, Y., Lavi, R., Kimbel, W.H., 1995. Hominid remains from Amud Cave in the context of the Levantine Middle Paleolithic. *Paléorient* 21, 47–60.

- Hummert, J.R., Van Gerven, D.P., 1985. Observations on the formation and persistence of radiopaque transverse lines. *Am. J. Phys. Anthropol.* 66, 297–306.
- Ishida, H., Kondo, O., 2002. The skull of the Neanderthal child No. 2. In: Akazawa, T., Muhesen, S. (Eds.), *Neanderthal Burials. Excavations of the Dederiyeh Cave, Afrin, Syria*. International Research Center for Japanese Studies, Kyoto, pp. 271–298.
- Kondo, O., Dodo, Y., 2002. The postcranial bones of the Neanderthal child of burial No. 1. In: Akazawa, T., Muhesen, S. (Eds.), *Neanderthal Burials. Excavations of the Dederiyeh Cave, Afrin, Syria*. International Research Center for Japanese Studies, Kyoto, pp. 139–214.
- Kondo, O., Ishida, H., 2002. The postcranial bones of the Neanderthal child of burial No. 2. In: Akazawa, T., Muhesen, S. (Eds.), *Neanderthal Burials. Excavations of the Dederiyeh Cave, Afrin, Syria*. International Research Center for Japanese Studies, Kyoto, pp. 299–322.
- Lewis, M., Roberts, C., 1997. Growing pains: the interpretation of stress indicators. *Int. J. Osteoarchaeol.* 7, 581–586.
- Liversidge, H.M., Molleson, T., 2004. Variation in crown and root formation and eruption of human deciduous teeth. *Am. J. Phys. Anthropol.* 123, 172–180.
- Macchiarelli, R., Bondioli, L., Censi, L., Hernaez, M.K., Salvadei, L., Sperduti, A., 1994. Intra- and interobserver concordance in scoring Harris lines: a test of bone sections and radiographs. *Am. J. Phys. Anthropol.* 95, 77–83.
- Madre-Dupouy, M., 1992. *L'Enfant du Roc de Marsal. Étude Analytique et Comparative*. Éditions du C.N.R.S., Paris.
- Mays, S.A., 1985. The relationship between Harris line formation and bone growth and development. *J. Archaeol. Sci.* 12, 207–220.
- McCown, T.D., Keith, A., 1939. *The Stone Age of Mount Carmel II: The Fossil Human Remains from the Levallois-Mousterian*. Clarendon Press, Oxford.
- Mercier, N., Valladas, H., 2003. Reassessment of TL age estimates of burnt flints from the Paleolithic site of Tabun Cave, Israel. *J. Hum. Evol.* 45, 401–409.
- Nagurka, M.L., Hayes, W.C., 1980. An interactive graphics package for calculating cross sectional properties of complex shapes. *J. Biomech.* 13, 59–64.
- O'Neill, M.C., Ruff, C.B., 2004. Estimating human long bone cross-sectional geometric properties: a comparison of noninvasive methods. *J. Hum. Evol.* 47, 221–235.
- Perkins Jr., D., 1964. Prehistoric fauna from Shanidar, Iraq. *Science* 144, 1555–1556.
- Rabinovich, R., Tchernov, E., 1995. Chronological, paleoecological and taphonomical aspects of the Middle Paleolithic site of Qafzeh, Israel. In: Buitenhuis, H., Uerpmann, H.P. (Eds.), *Archaeozoology of the Near East II*. Backhuys Publishers, Leiden, pp. 5–44.
- Reed, C.A., Braidwood, R.J., 1960. Toward a reconstruction of the environmental sequence in northeastern Iraq. In: Braidwood, R.J., Howe, B. (Eds.), *Prehistoric Investigations in Iraqi Kurdistan*. University of Chicago Press, Chicago, pp. 163–173.
- Ruff, C.B., 2003. Growth in bone strength, body size, and muscle size in a juvenile longitudinal sample. *Bone* 33, 317–329.
- Ruff, C.B., Trinkaus, E., Walker, A., Larsen, C.S., 1993. Postcranial robusticity in *Homo*, I: temporal trends and mechanical interpretations. *Am. J. Phys. Anthropol.* 91, 21–53.
- Ruff, C.B., Walker, A., Trinkaus, E., 1994. Postcranial robusticity in *Homo*, III: ontogeny. *Am. J. Phys. Anthropol.* 93, 35–54.
- Ruff, C.B., Trinkaus, E., Holliday, T.W., 2002. Body proportions and size. In: Zilhão, J., Trinkaus, E. (Eds.), *Portrait of the Artist as a Child. The Gravettian Human Skeleton from the Abrigo do Lagar Velho and Its Archeological Context*. Instituto Português de Arqueologia, Lisbon, pp. 365–391.
- Scheuer, L., Black, S., 2000. *Developmental Juvenile Osteology*. Academic Press, London.
- Shirley, M.M., 1963. The motor sequence. In: Dennis, W. (Ed.), *Readings in Child Psychology*. Prentice-Hall, Englewood Cliffs.
- Skinner, J.H., 1965. *The Flake Industries of Southwest Asia: A Typological Study*. Ph.D. Dissertation, Columbia University.
- Smith, B.H., 1991. Standards of human tooth formation and dental age assessment. In: Kelley, M.A., Larsen, C.S. (Eds.), *Advances in Dental Anthropology*. Wiley-Liss, New York, pp. 143–168.
- Solecki, R.S., 1963. Prehistory in Shanidar Valley, northern Iraq. *Science* 139, 179–193.
- Solecki, R.S., 1971. *Shanidar. The First Flower People*. Knopf, New York.
- Stefan, V.H., Trinkaus, E., 1998. Discrete trait and dental morphometric affinities of the Tabun 2 mandible. *J. Hum. Evol.* 34, 443–468.
- Suzuki, H., Takai, F. (Eds.), 1970. *The Amud Man and His Cave Site*. Academic Press of Japan, Tokyo.
- Tchernov, E., 1998. The faunal sequence of the southwest Asian Middle Paleolithic in relation to hominid dispersal events. In: Akazawa, T., Aoki, K., Bar Yosef, O. (Eds.), *Neandertals and Modern Humans in West Asia*. Plenum, New York, pp. 77–90.
- Tillier, A.M., 1999. *Les Enfants Moustériens de Qafzeh. Interprétation Phylogénétique et Paléoaurologique*. CNRS Éditions, Paris.
- Tompkins, R.L., Trinkaus, E., 1987. La Ferrassie 6 and the development of Neandertal pubic morphology. *Am. J. Phys. Anthropol.* 73, 233–239.
- Trinkaus, E., 1981. Neandertal limb proportions and cold adaptation. In: Stringer, C.B. (Ed.), *Aspects of Human Evolution*. Taylor & Francis, London, pp. 187–219.
- Trinkaus, E., 1983. *The Shanidar Neandertals*. Academic Press, New York.
- Trinkaus, E., 1984. Western Asia. In: Smith, F.H., Spencer, F. (Eds.), *The Origins of Modern Humans: A World Survey of the Fossil Evidence*. Alan R. Liss, New York, pp. 251–293.
- Trinkaus, E., 1995. Near Eastern late archaic humans. *Paléorient* 21, 9–23.
- Trinkaus, E., 2006. Body length and body mass. In: Trinkaus, E., Svoboda, J.A. (Eds.), *Early Modern Human Evolution in Central Europe: The People of Dolní Věstonice and Pavlov*. Oxford University Press, New York, pp. 233–241.
- Trinkaus, E., Churchill, S.E., Ruff, C.B., 1994. Postcranial robusticity in *Homo*, II: humeral bilateral asymmetry and bone plasticity. *Am. J. Phys. Anthropol.* 93, 1–34.
- Trinkaus, E., Ruff, C.B., 1996. Early modern human remains from eastern Asia: the Yamashita-cho 1 immature postcrania. *J. Hum. Evol.* 30, 299–314.
- Trinkaus, E., Ruff, C.B., 1999a. Diaphyseal cross-sectional geometry of Near Eastern Middle Paleolithic humans: the femur. *J. Archaeol. Sci.* 26, 409–424.
- Trinkaus, E., Ruff, C.B., 1999b. Diaphyseal cross-sectional geometry of Near Eastern Middle Paleolithic humans: the tibia. *J. Archaeol. Sci.* 26, 1289–1300.
- Trinkaus, E., Ruff, C.B., 2000. Comment on: O.M. Pearson, "Activity, climate, and postcranial robusticity. Implications for modern human origins and scenarios of adaptive change." *Curr. Anthropol.* 41, 598.
- Trinkaus, E., Ruff, C.B., Esteves, F., Santos Coelho, J.M., Silva, M., Mendonça, M., 2002a. The lower limb remains. In: Zilhão, J., Trinkaus, E. (Eds.), *Portrait of the Artist as a Child. The Gravettian Human Skeleton from the Abrigo do Lagar Velho and Its Archeological Context*. Instituto Português de Arqueologia, Lisbon, pp. 435–465.
- Trinkaus, E., Hillson, S.W., Santos Coelho, J.M., 2002b. Paleopathology. In: Zilhão, J., Trinkaus, E. (Eds.), *Portrait of the Artist as a Child. The Gravettian Human Skeleton from the Abrigo do Lagar Velho and Its Archeological Context*. Instituto Português de Arqueologia, Lisbon, pp. 489–495.
- Valladas, H., Joron, J.L., Valladas, G., Arensburg, B., Bar-Yosef, O., Belfer-Cohen, A., Goldberg, P., Laville, H., Meignan, L., Rak, Y., Tchernov, E., Tillier, A.M., Vandermeersch, B., 1987. Thermoluminescence dates for the Neanderthal burial site at Kebara in Israel. *Nature* 330, 159–160.
- Valladas, H., Mercier, N., Froget, L., Hovers, E., Joron, J.L., Kimbel, W.H., Rak, Y., 1999. TL dates for the Neanderthal site of the Amud Cave, Israel. *J. Archaeol. Sci.* 26, 259–268.
- Vandermeersch, B., 1981. *Les Hommes Fossiles de Qafzeh (Israël)*. C.N.R.S., Paris.
- Vlček, E., 1973. Postcranial skeleton of a Neanderthal child from Kiik-Koba, U.S.S.R. *J. Hum. Evol.* 2, 537–544.
- Vogel, J.C., Waterbolk, H.T., 1963. Groningen radiocarbon dates IV. *Radiocarbon* 5, 163–202.
- Zeder, M.A., 2005. New perspectives on livestock domestication in the Fertile Crescent as viewed from the Zagros Mountains. In: Vigne, J.-D., Peters, J., Helmer, D. (Eds.), *The First Steps of Animal Domestication: New Archaeozoological Approaches*. Oxbow Press, Oxford, pp. 125–147.
- Zeder, M.A., 2006. A critical examination of markers of initial domestication in goats (*Capra hircus*). In: Zeder, M.A., Bradley, D.G., Emshwiller, E., Smith, B.D. (Eds.), *Documenting Domestication: New Genetic and Archaeological Paradigms*. University of California Press, Berkeley, pp. 180–208.